

Study of the $\bar{p}d \rightarrow \bar{p}pn$ and $\bar{p}n \rightarrow \bar{p}n$ reactions at 5.55 GeV/c

H. Braun, D. Brick, A. Fridman, J.-P. Gerber, E. Jegham, P. Juillot, and C. Voltolini
Groupe des Chambres à Bulles à Hydrogène, Centre de Recherches Nucléaires, Strasbourg, France

(Received 27 June 1974)

From a 150 000-photograph exposure, we analyzed the $\bar{p}d \rightarrow \bar{p}p_s n$ reaction, p_s denoting a proton stopping in the deuterium-filled bubble chamber. Choosing kinematical regions in which the p_s can be recognized as a spectator, we studied the $\bar{p}n \rightarrow \bar{p}n$ process. From the observed $\bar{p}n$ diffraction peak, we obtained an exponential slope for the four-momentum-transfer distribution of $b_n = 9.4 \pm 0.8$ (GeV/c)⁻², the elastic $\bar{p}n$ cross section being estimated as $\sigma_e(\bar{p}n) = 16.5 \pm 2.4$ mb. The present values in conjunction with those obtained at ≈ 1.8 and 3.5 GeV/c show that in this region b_n and $\sigma_e(\bar{p}n)$ decrease with increasing incident momentum. We compared our data with the reactions $np \rightarrow np$ at ≈ 5.4 GeV/c and $\bar{p}p \rightarrow \bar{p}p$ at 5.7 GeV/c. The $\bar{p}n \rightarrow \bar{p}n$ and $np \rightarrow np$ differential cross sections exhibit a crossover phenomenon while $\bar{p}p$ and $\bar{p}n$ elastic scatterings show an isospin dependence. We also analyzed the $\bar{p}d \rightarrow \bar{p}p_s n$ reaction by means of the Glauber formalism.

I. INTRODUCTION

In this paper we study the breakup reaction $\bar{p}d \rightarrow \bar{p}pn$ at 5.55 GeV/c incident momentum. The experiment was accomplished using 150 000 photographs taken at the ZGS with the 30-in. deuterium-filled bubble chamber. The present data were extracted from the two-pronged events having their positive outgoing track stopping in the chamber. We will, therefore, denote the studied reaction by $\bar{p}d \rightarrow \bar{p}p_s n$, where p_s is considered here as being a stopping proton.

In the next section we discuss briefly the experimental procedure as well as some of our sampling problems. We give some details on the difficulty of isolating one-constraint fits from the two-pronged events at 5.55 GeV/c. Nevertheless we succeed to obtain a number of events still sufficient to give information about $\bar{p}n \rightarrow \bar{p}n$ scattering as will be shown in Sec. III. We studied this elastic scattering process by choosing kinematical regions for the $\bar{p}d \rightarrow \bar{p}p_s n$ reaction in which the p_s has a high probability of being a spectator.

We also analyzed the $\bar{p}d \rightarrow \bar{p}p_s n$ reaction by means of the Glauber formalism (Sec. IV). To do this, we attempted to take into account the fact that we have only a subsample of all of the breakup reactions, namely, those having outgoing protons which stop in the chamber. The conclusions of the present work are presented in Sec. V.

II. EXPERIMENTAL PROCEDURE

The film was scanned for the two-pronged events in which the positive track stops in the chamber. No cut on the length of the stopping track was imposed. After the kinematical fitting of the events, a considerable number of those which fitted the $\bar{p}d \rightarrow \bar{p}p_s n$ reaction also gave fits with other hypoth-

eses. The ambiguity between the various reactions was resolved on the basis of missing-mass criteria taking into account the errors on these quantities. In fact, a detailed investigation has shown that the use of the proposed criteria is nearly equivalent to rejecting the events having a χ^2 probability less than 0.35 for the fit to the reaction $\bar{p}d \rightarrow \bar{p}p_s n$. This cut is a consequence of the difficulty of isolating one-constraint fits from the two-pronged events at 5.55 GeV/c incident momentum. Furthermore, the same χ^2 probability limit has the advantage of cleaning up the sample of events fitting only the reaction $\bar{p}d \rightarrow \bar{p}p_s n$. This sample, indeed, appears to be strongly contaminated by channels having more than one neutral particle in the final state. For these reasons, we applied a 0.35 χ^2 probability cut to all of the events fitting the $\bar{p}d \rightarrow \bar{p}pn$ hypothesis, obtaining thus 3839 events. An additional cut, made on the missing mass squared, gave us finally 3727 events which we consider as being a clean sample of $\bar{p}d \rightarrow \bar{p}p_s n$ events.

A considerable part of the events contained in the film were lost during the scanning and measuring processes because of short, or steeply dipping, outgoing p_s tracks. We distinguish here essentially two sources of losses considered for simplicity as being independent. They are

(1) the losses due to events which had short p_s tracks and which were not recorded during the scanning or could not be measured successfully, and

(2) the losses due to the scanning efficiency of the operators.

The losses of the type (1) were estimated by studying the azimuthal distributions of the p_s tracks around the incident \bar{p} beam for different laboratory momentum bands of the p_s . From the lack of isotropy of these distributions, we esti-

mated the weights by which one has to multiply the number of events in each p_s momentum band in order to compensate for the losses. The distribution of these weights [$w(P_s)$] as a function of P_s , the p_s laboratory momentum, is displayed in Fig. 1. This distribution is basically hyperbolic in nature although it tends to increase slightly for large P_s . This small tendency is simply due to the geometry of the chamber, which has a depth much smaller than its width. Additional losses will then occur for high P_s when the p_s are emitted nearly perpendicularly to the plane of the camera. Fitting the weight distribution with a hyperbolic function and a one-parameter parabola in order to describe the small rise of w toward high P_s , we obtained the fitted curve shown in Fig. 1. This curve will be used to weight each event individual-

ly. The correction for losses due to the scanning efficiency of the scanners [(2)] was obtained from two separate scans of the film. This enabled us to calculate the scanning efficiency ϵ as a function of P_s . The quantity $1/\epsilon$ was then used as an additional weight. In other words, each event contributing to the distributions examined below was weighted by its corresponding w/ϵ value.

In order to avoid events with too-high w/ϵ values, for which the proposed correction might not be really meaningful (see Fig. 1), we rejected all the events having $P_s \leq 0.1$ GeV/c. We obtained thus 3434 events which correspond to 4430 weighted events. It is this sample of 3434 events which will be utilized for the present analysis.

III. STUDY OF THE ELASTIC $\bar{p}n \rightarrow \bar{p}n$ SCATTERING

For studying the $\bar{p}n \rightarrow \bar{p}n$ process, we will extract from our 3434 $\bar{p}d \rightarrow \bar{p}p_s n$ events a subsample in which the p_s can be considered as being, most likely, a spectator proton. In contrast to other inelastic $\bar{p}d$ reactions, the outgoing nucleon of lower momentum cannot be considered as a spectator nucleon for the breakup reaction. This is because the $\bar{p}N$ elastic scattering in the 5.5 GeV/c region is dominated by diffractive scattering, namely, the \bar{p} is scattered with small momentum transfer. The recoiling nucleon has then a laboratory momentum comparable in magnitude to the Fermi momentum of the nucleons inside the deuteron. Apart from this intrinsic difficulty, further complications are introduced in the $\bar{p}d \rightarrow \bar{p}p_n$ reaction by double-scattering terms and interference phenomena.¹ There is thus no way, based on kinematical arguments, of identifying which of the outgoing nucleons is the spectator. Assignment of the spectator nucleon can only be made on the basis of probability arguments. To

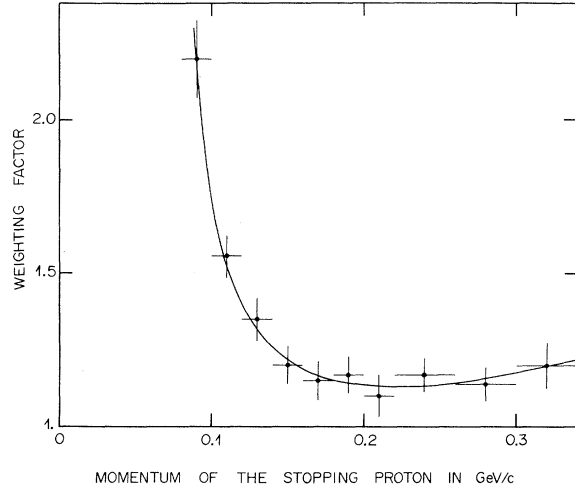


FIG. 1. Weighting factor as a function of P_s , the laboratory momentum of the stopping proton. The curve represents the fit to our data (see text).

do this, we will define a kinematical region for the $\bar{p}d \rightarrow \bar{p}p_s n$ reaction in which the p_s (n) has a high (low) probability of being a spectator nucleon.

We will essentially consider two methods. In the first one, we will select events where the laboratory momentum P_s is smaller than 0.23 GeV/c while the momentum of the outgoing n (P_n) is taken as being greater than 0.25 GeV/c. This event selection gives a sample with a small probability of having a spectator neutron. Using the Hulthén wave function for describing the deuteron, this probability is estimated to be 0.01. Similarly, the P_s have a high probability of being spectators since 95% of them are predicted by the Hulthén distribution to have a momentum smaller than 0.23 GeV/c. In fact, the P_s and P_n cuts were chosen in such a way that one may obtain a good agreement between the momentum and angular distributions of the p_s and the Hulthén wave-function predictions. As can be seen from Fig. 2, the p_s angular distribution shows roughly the expected isotropical behavior while the P_s distribution is well represented by the curve shown in this figure. This curve, which is calculated by a Monte Carlo method, is the Hulthén prediction modified by our selection criteria. The same calculation also shows that the isotropy of the angular distribution is not greatly affected by our event selection.

The second selection method is based on a slightly more quantitative approach. We associated to each outgoing nucleon a probability W_N of being a spectator. These probabilities are calculated from the expression

$$W_N = \int_{\vec{P}_N} |\Phi(\vec{P}_N)|^2 d\vec{P}_N,$$

where \vec{P}_N is the laboratory momentum of the outgoing nucleon N and $\Phi(\vec{P}_N)$ the Hulthén wave function. We chose to define as events having a spectator proton in the final state those which satisfy the inequality

$$\frac{W_n}{W_p + W_n} < 0.15.$$

In the same manner as above, this cut was chosen in order to have a good agreement between the experimental results and the Hulthén predictions for the p_s (Fig. 2). Both methods lead to a comparable number of events and also to practically identical distributions for t , the four-momentum transfer between the incident and outgoing \bar{p} (see Fig. 3). Indeed, by fitting the t distributions of Fig. 3 in the interval $0.1 < |t| < 0.4$ (GeV/c)² with $e^{b_n t}$ functions, one obtains nearly the same slopes, i.e., 9.9 ± 0.8 and 8.9 ± 0.8 (GeV/c)⁻² for Figs. 3(a) and 3(b), respectively. We consider the average value [9.4 ± 0.8 (GeV/c)⁻²] as the slope characterizing our $\bar{p}n$ diffraction peak.

One notices that these values are compatible with those found by analyzing the $\bar{p}d \rightarrow \bar{p}d$ scattering obtained from the same experiment.² Indeed, by fitting these data with an expression deduced from the Glauber formalism, we were able to determine a $b_n = 9.2 \pm 0.8$ (GeV/c)⁻² value.² This last fact and the rather good agreement observed between the Hulthén predictions and the experimental distributions of the p_s give us some confidence in the method used for isolating the $\bar{p}n \rightarrow \bar{p}n$ channel. These methods are, however, not very efficient, since from a sample of 3434 events only ≈ 400

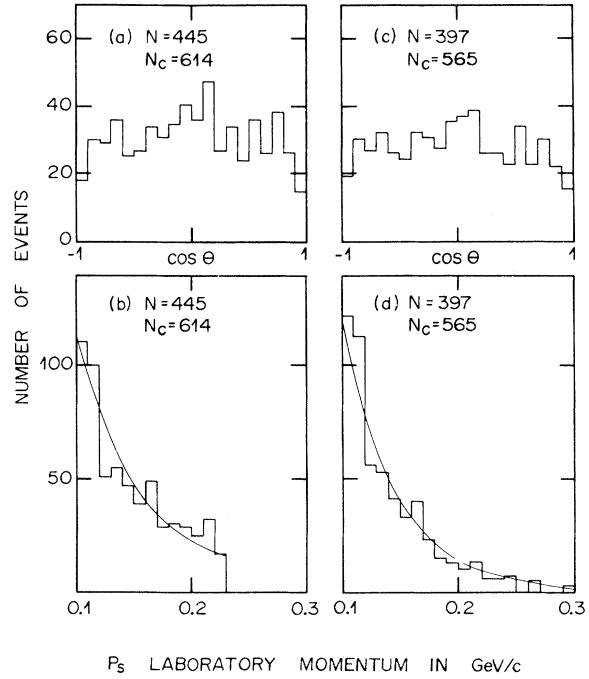


FIG. 2. Weighted angular and momentum distributions of the p_s in the laboratory system. The p_s emission angle θ is defined with respect to the incoming \bar{p} direction. N and N_c represent the numbers of true and weighted events, respectively. In (a) and (b) the events were selected by the $P_s \leq 0.23$ GeV/c and $P_n > 0.25$ GeV/c criteria, while in (c) and (d) the $W_n / (W_n + W_p) < 0.15$ condition was used (see text). The solid curves represent the Hulthén wave-function predictions modified by our selection.

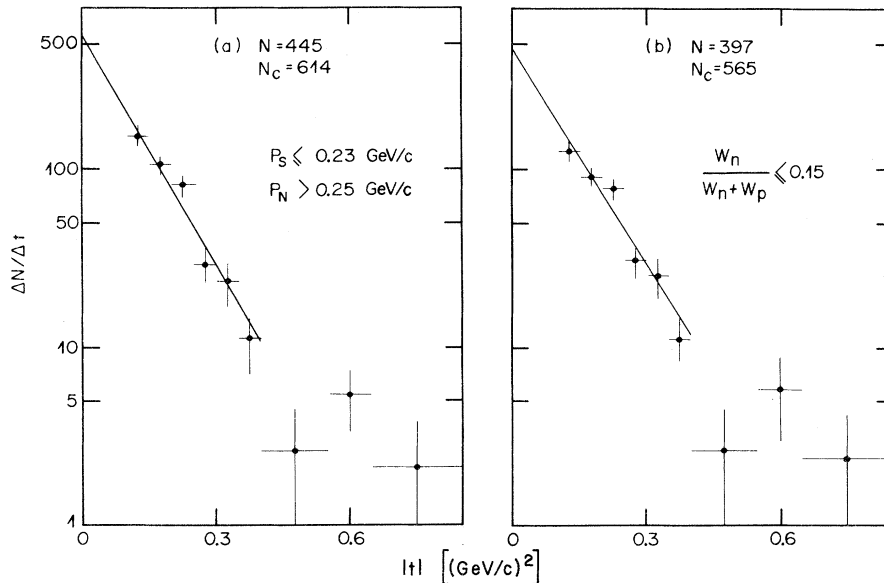


FIG. 3. Weighted four-momentum-transfer distributions for the $\bar{p}n \rightarrow \bar{p}n$ events selected according to the two methods described in the text. N and N_c represent the numbers of true and weighted events, respectively. The curves represent exponential fits to our data in the range $0.1 \leq |t| < 0.4$ (GeV/c)².

were accepted as being $\bar{p}n$ elastic scatters. Moreover, the event selection used above introduces a minimum value in the $|t|$ distributions as shown by Fig. 3.

Because of our event selection, the elastic $\bar{p}n$ cross section $[\sigma_e(\bar{p}n)]$ cannot be determined directly from the present experiment. If, however, one neglects the real part of the elastic $\bar{p}n$ scattering amplitude at $t=0$, the optical theorem gives a measure of $\sigma_e(\bar{p}n)$ providing the total $\bar{p}n$ cross section $[\sigma_t(\bar{p}n)]$ is known. Although the real part of the $\bar{p}n$ amplitude is not known at 5.5 GeV/c, it is expected to have a small value.³ Using the exponential form of the $\bar{p}n \rightarrow \bar{p}n$ differential cross section, one has

$$\frac{d\sigma}{dt} = \frac{[\sigma_t(\bar{p}n)]^2}{16\pi} e^{b_n t},$$

from which one obtains the relation

$$\sigma_e(\bar{p}n) = \frac{[\sigma_t(\bar{p}n)]^2}{16\pi} \frac{1}{b_n}.$$

The $\sigma_t(\bar{p}n)$ can be calculated from the well-known Glauber formula¹:

$$\sigma_t(\bar{p}d) = \sigma_t(\bar{p}p) + \sigma_t(\bar{p}n) - \delta\sigma,$$

where the cross-section defect is given by^{1,4}

$$\delta\sigma = \frac{\langle r^{-2} \rangle}{4\pi} \left\{ \sigma_t(\bar{p}p)\sigma_t(\bar{p}n) - \frac{1}{2}[\sigma_t(\bar{p}p) - \sigma_t(\bar{p}n)]^2 \right\}.$$

We have used for the average inverse square of the neutron-proton distance the value $\langle r^{-2} \rangle = 0.0327 \pm 0.004 \text{ mb}^{-1}$ which was interpolated from the existing data.^{5,6} For the total $\bar{p}d$ and $\bar{p}p$ cross sections we took the values $\sigma_t(\bar{p}d) = 109 \pm 1.5 \text{ mb}$ (Ref. 7) and $\sigma_t(\bar{p}p) = 63.6 \pm 1.4 \text{ mb}$,⁸ respectively. This gives us a total $\bar{p}n$ cross section of $55 \pm 3 \text{ mb}$, where the uncertainty in $\langle r^{-2} \rangle$ is only responsible for 0.3 mb in the above quoted error. This latter value and the slope b_n determined from our data give us finally an elastic $\bar{p}n$ cross section of $\sigma_e(\bar{p}n) = 16.5 \pm 2.4 \text{ mb}$. Here also the uncertainty in $\langle r^{-2} \rangle$ is responsible for only a small part of the error, i.e., $\approx 0.2 \text{ mb}$. In Table I we compare the slopes b_n and the $\sigma_e(\bar{p}n)$ cross sections obtained from recent $\bar{p}d$ data. Although the data are rather sparse, it appears that $\sigma_e(\bar{p}n)$ and b_n tend to decrease with increasing incident momentum.

The large error found for $\sigma_e(\bar{p}n)$ does not permit

TABLE I. Variation of the elastic $\bar{p}n \rightarrow \bar{p}n$ cross section $[\sigma_e(\bar{p}n)]$ and of the slope (b_n) of the diffraction peak as a function of incident momentum.

Momentum (GeV/c)	$\sigma_e(\bar{p}n)$ (mb)	$ t $ range used for fitting b_n [(GeV/c) ²]	Slope b_n [(GeV/c) ⁻²]
$\approx 1.8^a$	29.3 ± 1.7	< 0.3	14.9 ± 0.6
3.5^b	20.6 ± 2.0	$0.15 - 0.40$	11.8 ± 0.4
5.5^c	16.5 ± 2.4	$0.1 - 0.4$	9.4 ± 0.8

^aSee Ref. 11.

^bSee Ref. 12.

^cThis experiment.

us to detect by comparing $\sigma_e(\bar{p}n)$ with $\sigma_e(\bar{p}p)$ an isospin dependence of the $\bar{N}N - \bar{N}N$ scattering. These values are very close to each other [$\sigma_e(\bar{p}n) = 16.5 \pm 2.4 \text{ mb}$; $\sigma_e(\bar{p}p) = 16.3 \pm 0.6 \text{ mb}$ (see Ref. 8)] and need, hence, a better determination. However, the difference observed in the slopes $b_p = 13 \pm 1.5 \text{ (GeV/c)}^{-2}$ (see Ref. 9) and $b_n = 9.4 \pm 0.8 \text{ (GeV/c)}^{-2}$ suggests such an isospin dependence as noted at smaller incident momenta.¹⁰⁻¹² This is even more striking if the $\bar{p}n$ and $\bar{p}p$ total cross sections are compared at 5.5 GeV/c. These values, $\sigma_t(\bar{p}n) = 55 \pm 3 \text{ mb}$ and $\sigma_t(\bar{p}p) = 63.6 \pm 1.4 \text{ mb}$, predict by use of the optical theorem a significant difference in the $\bar{p}n$ and $\bar{p}p$ differential cross section at $t=0$.

As pointed out in a previous paper,² a crossover phenomenon is observed when we compare the $\bar{p}n$ and p_n differential cross sections at $\approx 5.5 \text{ GeV/c}$. Using the $np \rightarrow np$ data at 5.36–5.87 GeV/c,¹³ one obtains a crossover point at the square of the four-momentum transfer $-t_c = 0.15 \pm 0.09 \text{ (GeV/c)}^2$. This value has the same order of magnitude as that found at 3.5 GeV/c (see Ref. 12) [$-t_c \approx 0.15 \text{ (GeV/c)}^2$] and that obtained by comparing the $\bar{p}p \rightarrow \bar{p}p$ reaction with $p_p \rightarrow p_p$ at 5.5 GeV/c (see Ref. 2) [$-t_c = 0.18 \pm 0.02 \text{ (GeV/c)}^2$].

IV. ANALYSIS OF THE $\bar{p}d \rightarrow \bar{p}p_n$ REACTION

In this section we will study the breakup reaction $\bar{p}d \rightarrow \bar{p}p_n$. According to the Glauber multiple-scattering theory, the differential cross section $d\sigma/dt$ can be written as¹

$$\begin{aligned} \frac{d\sigma}{dt} = & \frac{\pi}{k^2} \left([1 - S^2(\frac{1}{2}\bar{q})][|f_n(\bar{q})|^2 + |f_p(\bar{q})|^2] + 2[S(\bar{q}) - S^2(\frac{1}{2}\bar{q})]\text{Re}[f_n(\bar{q})f_p^*(\bar{q})] \right. \\ & + \frac{1}{\pi k} \text{Im} \left\{ f_n^*(\bar{q}) \int [S(\frac{1}{2}\bar{q})S(\bar{q}') - S(\bar{q}' - \frac{1}{2}\bar{q})] f_n(\frac{1}{2}\bar{q} + \bar{q}') f_p(\frac{1}{2}\bar{q} - \bar{q}') d^2q' \right\} \\ & + \frac{1}{\pi k} \text{Im} \left\{ f_p^*(\bar{q}) \int [S(\frac{1}{2}\bar{q})S(\bar{q}') - S(\bar{q}' + \frac{1}{2}\bar{q})] f_n(\frac{1}{2}\bar{q} + \bar{q}') f_p(\frac{1}{2}\bar{q} - \bar{q}') d^2q' \right\} \\ & \left. + \frac{1}{(2\pi k)^2} \iint [S(\bar{q}' - \bar{q}'') - S(\bar{q}')S(\bar{q}'')] f_n(\frac{1}{2}\bar{q} + \bar{q}') f_p(\frac{1}{2}\bar{q} - \bar{q}') f_p^*(\frac{1}{2}\bar{q} + \bar{q}'') f_n^*(\frac{1}{2}\bar{q} - \bar{q}'') d^2q' d^2q'' \right). \quad (1) \end{aligned}$$

Here, the $f_N(\vec{q})$ represent the free $\bar{p}N$ elastic-scattering amplitudes, and $S(\vec{q})$ represents the deuteron form factor, while k is the laboratory momentum of the incident particle. The argument \vec{q} in these functions is the three-momentum transfer between the incident and outgoing \bar{p} expressed in the laboratory system. By virtue of the small-scattering-angle approximation used for deriving the above formula, one generally considers that $t = -q^2$. This is, in any case, verified by the present data, for which the $|t|$ and q^2 distributions are nearly identical. For comparing our data with formula (1), we have to take into account the fact that we have only a subsample of breakup reactions, namely those having their outgoing proton stopping in the chamber.

In the framework of the first-order impulse approximation [which corresponds to neglecting all the terms in formula (1) containing an integral], a correction for our event selection can be made rather easily. This is based on the fact that in this case the reaction results from the single scattering of the incident particles on the bound nucleons contained in the deuteron. Then our losses are taken into account by replacing $f_{p,n}(\vec{q})$ by $K_{p,n}f_{p,n}(\vec{q})$ in the first-order impulse approximation of $d\sigma/dt$ where $0 \leq K_{p,n} \leq 1$. The factor K_n represents simply the fraction of $\bar{p}n$ elastic-scattering events with a visible spectator proton, i.e., corresponding to $0.1 \leq P_s \leq 0.3$ GeV/c. Thus, on the basis of Hulthén wave function, K_n will be of the order of 0.6. Similarly, our event selection also leads to losses for the $\bar{p}p$ elastic-scattering contribution. If we neglect the Fermi motion of the proton target in the process $\bar{p}p \rightarrow \bar{p}p$, our P_s range will correspond to an interval of $0.01 \leq |t| \leq 0.09$ (GeV/c)². Then K_p will have a value of 1 in this interval and 0 elsewhere.

Such a simple picture cannot, of course, be applied to the terms arising from the double scattering process. By using formula (1) we will therefore correct only the $f_N(\vec{q})$ entering in the single-scattering terms, including those due to interferences with double-scattering processes. In other words, all the $f_N(\vec{q})$ which do not appear in the various integrals of formula (1) are replaced by $K_N f_N(\vec{q})$. The present approach may be justified by the fact that the double-scattering contribution to the $\bar{p}d \rightarrow \bar{p}pn$ reaction is expected to be small. Indeed, this contribution, which is calculated from the ratio

$$R = \left[\left(\frac{d\sigma}{dt} \right)_{S+D} - \left(\frac{d\sigma}{dt} \right)_{S,D} \right] / \left(\frac{d\sigma}{dt} \right)_{S+D},$$

appears to have a nearly constant percentage of about 12% in the t range available in the present data. The index S ($S+D$) indicates that the $\bar{p}d$

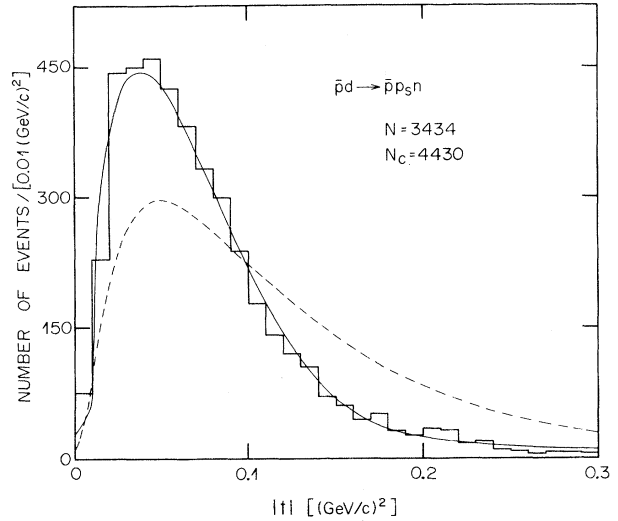


FIG. 4. Weighted distribution of the four-momentum transfer between the incident and outgoing \bar{p} . N and N_c represent the numbers of true and weighted events, respectively. The solid curve represents the distribution obtained by fitting the Glauber formula taking into account our correction factors (see text), while the dashed line is the prediction of the uncorrected Glauber model normalized to N_c .

$\rightarrow \bar{p}pn$ differential cross section is calculated by neglecting (taking into account) the double-scattering contribution. The $R \approx 0.12$ value was obtained by using formula (1) and purely imaginary scattering amplitudes of the form

$$f_N(\vec{q}) = i f_N^0 e^{b_N t / 2}.$$

The b_p and f_p^0 quantities were taken from free $\bar{p}p$ elastic-scattering data using $b_p = 13 \pm 1.5$ (GeV/c)⁻² (see Ref. 9) and the optical theorem $f_p^0 = k \sigma_t(\bar{p}p) / 4\pi$ with $\sigma_t(\bar{p}p) = 63.6 \pm 1.4$ mb.⁹ For b_n and $f_n^0 = k \sigma_t(\bar{p}n) / 4\pi$ we took the values determined in the previous section. The form factor we utilized was deduced from the Hulthén wave function. However, in order to evaluate the various integrals appearing in (1), we used the more convenient $S(\vec{q}) = \exp(-\alpha q^2)$ form with $\alpha = 34$ (GeV/c)⁻². This value was adjusted in Ref. 2, in which the $\bar{p}d \rightarrow \bar{p}d$ process obtained from the same experiment was studied.

Using the $f_N(\vec{q})$ and $S(\vec{q})$ defined above we fitted formula (1) to our experimental t distribution displayed in Fig. 4. This was achieved by introducing the K_N correction factors in formula (1) as described above. We consider K_n as a free parameter, while K_p is assumed to have a nonzero value ($K_p = 1$) in the interval $0.01 \leq |t| < t_0$ (GeV/c)². From the previous reasoning the upper limit t_0 will be of the order of 0.09 (GeV/c)². However, as this limit is not well defined (among other things, because of our scanning criteria), we determined t_0 from

our fit. To achieve this we approximated for $|t| \geq 0.01$ (GeV/c)² the K_p step function by

$$K_p = \left[1 + \exp\left(\frac{|t| - t_0}{\beta t_0}\right) \right]^{-1},$$

β being an additional free parameter. From our fit we obtained $K_n = 0.43 \pm 0.03$, $t_0 = 0.15 \pm 0.01$ (GeV/c)², and $\beta = 0.27 \pm 0.04$, the two former values having the expected order of magnitude. The fitted distribution represented by the solid line in Fig. 4 gives a good description of our data. For comparison we also show the distribution (dashed curve) obtained when we do not take into account the K_n and K_p correction factors. This function, which is calculated with the same $f_N(\vec{q})$ as defined above, is not able to reproduce the experimental distribution. This shows that, in any case, the introduction of the proposed correction factors is essential to describe our data. Furthermore, the reasonable values found for K_n and t_0 give us some confidence in the method used to take into account our event selection.

V. CONCLUSIONS

From the 3434 $\bar{p}d \rightarrow \bar{p}p_s n$ events obtained at 5.55 GeV/c, we extracted a small subsample of events (≈ 400) in which the p_s could be recognized as a spectator proton. This allowed us to study the $\bar{p}n \rightarrow \bar{p}n$ differential cross section, for which we found the exponential slope of the diffraction peak to be $b_n = 9.4 \pm 0.8$ (GeV/c)⁻². It is worthwhile to note that this value is equal to that obtained by ana-

lyzing the $\bar{p}d \rightarrow \bar{p}d$ reaction at 5.55 GeV/c by means of the Glauber formalism.

Assuming that the real part of the $\bar{N}N$ elastic scattering amplitude is negligible at $t=0$, we were able to estimate the $\bar{p}n$ elastic cross section to be $\sigma_e(\bar{p}n) = 16.5 \pm 2.4$ mb. If we compare our result with those found at ≈ 1.8 and 3.5 GeV/c, it appears that $\sigma_e(\bar{p}n)$ and b_n tend to decrease with increasing incident momentum.

As noted previously at lower incident momenta, we also detected an isospin dependence for the $\bar{N}N \rightarrow \bar{N}N$ scattering. This is shown by differences observed in the elastic differential cross sections of $\bar{p}n \rightarrow \bar{p}n$ (5.5 GeV/c) and $\bar{p}p \rightarrow \bar{p}p$ (5.7 GeV/c) at nearly the same incident momentum. Furthermore, the present data when compared to the $np \rightarrow np$ scattering at ≈ 5.4 GeV/c exhibit a crossover phenomenon at a four-momentum transfer $-t_c = 0.15 \pm 0.09$ (GeV/c)². One observes that this value is nearly equal to that observed at 3.5 GeV/c and to the crossover point obtained by comparing the $\bar{p}p \rightarrow \bar{p}p$ and $pp \rightarrow pp$ reactions at 5.7 and 5.5 GeV/c, respectively.

We also studied the $\bar{p}d \rightarrow \bar{p}p_s n$ reaction by means of the Glauber formalism, taking into account that we used here only a subsample of breakup reactions. This was achieved by introducing correction factors in the first-order impulse-approximation part of the expression giving the elastic differential cross section. By fitting this expression to our data we obtain reasonable values for the correction factors and a good description of the $\bar{p}d \rightarrow \bar{p}p_s n$ differential cross section.

¹V. Franco and R. J. Glauber, Phys. Rev. **142**, 1195 (1966).

²H. Braun, A. Fridman, E. Jegham, P. Juillot, J. A. Malko, C. Voltolini, G. R. Charlton, W. A. Cooper, and B. Musgrave, Nucl. Phys. **B54**, 61 (1973).

³As the real part of $\bar{p}p$ scattering at $t=0$ is predicted to have a small value [see, for instance, A. Tavkhelidze, in *High Energy Physics*, proceedings of the Fifteenth International Conference on High Energy Physics, Kiev, 1970, edited by V. Shelest (Naukova Dumka, Kiev, U.S.S.R., 1972)] we assumed that this is also true for the $\bar{p}n \rightarrow \bar{p}n$ scattering.

⁴C. Wilkin, Phys. Rev. Lett. **17**, 561 (1966).

⁵R. L. Cool, G. Giacomelli, T. F. Kycia, B. A. Leontic, K. K. Li, A. Lundby, J. Teiger, and C. Wilkin, Phys. Rev. D **1**, 1887 (1970).

⁶Yu. P. Gorin *et al.*, Serpukhov Report No. IHEP 71-100 (unpublished).

⁷This value is obtained by interpolation of the existing data. See, for instance, Ref. 2.

⁸K. Böckmann *et al.*, Nuovo Cimento **42A**, 954 (1966).

⁹This value was obtained by interpolating the existing slopes b_n compiled in Ref. 2.

¹⁰J. Berryhill and D. Cline, Phys. Rev. Lett. **21**, 770 (1968).

¹¹Z. Ming Ma and G. A. Smith, Phys. Rev. Lett. **28**, 779 (1972).

¹²B. G. Reynolds, K. E. Weaver, J. M. Bishop, D. O. Huwe, and J. A. Malko, Phys. Rev. D **2**, 1767 (1970).

¹³M. L. Perl, J. Cox, M. J. Longo, and M. N. Kreisler, SLAC Report No. SLAC-PUB-622, 1969 (unpublished).